doi:10.1016/j.jmb.2008.07.030 *J. Mol. Biol.* (2008) **382**, 327–341

JMB

Available online at www.sciencedirect.com

ScienceDirect

ELSEVIER

Mechanistic Basis of Zidovudine Hypersusceptibility and Lamivudine Resistance Conferred by the Deletion of Codon 69 in the HIV-1 Reverse Transcriptase Coding Region

Mónica Kisic[1], Jesús Mendieta[1], María C. Puertas[2], Mariona Parera[2], Miguel A. Martínez[2], Javier Martinez-Picado[2,3] and Luis Menéndez-Arias[1]*

[1]*Centro de Biología Molecular "Severo Ochoa," Consejo Superior de Investigaciones Científicas and Universidad Autónoma de Madrid, 28049 Madrid, Spain*

[2]*Laboratori de Retrovirologia, Fundació irsiCaixa, Hospital Universitari Germans Trias i Pujol, Badalona, 08916 Barcelona, Spain*

[3]*Institució Catalana de Recerca i Estudis Avançats (ICREA), Barcelona, Spain*

Received 29 May 2008; received in revised form 10 July 2008; accepted 14 July 2008
Available online 17 July 2008

Deletions in the β3–β4 hairpin loop of human immunodeficiency virus type 1 reverse transcriptase (RT) are associated with the emergence of multidrug resistance. Common mutational patterns involve the deletion of Asp67 (Δ67) and mutations such as K70R and T215F or T215Y, or the deletion of Thr69 (Δ69) and mutations of the Q151M complex. Human immunodeficiency virus type 1 clones containing Δ69 in a multidrug-resistant sequence background, including the Q151M complex and substitutions K103N, Y181C, M184V, and G190A, showed high-level resistance to all tested nucleoside RT inhibitors. In a multidrug-resistant sequence context, the deletion increases viral replication capacity. By itself, Δ69 conferred increased susceptibility to β-D-(+)-3′-azido-3′-deoxythymidine (AZT) and β-L-(−)-2′,3′-dideoxy-3′-thiacytidine resistance. Here, we use transient kinetics to show that, in a wild-type sequence background, Δ69 does not affect the discrimination between AZT triphosphate and 2′-deoxythymidine 5′-triphosphate, but decreases the catalytic efficiency of the incorporation of β-L-(−)-2′,3′-dideoxy-3′-thiacytidine triphosphate relative to 2′-deoxycytidine 5′-triphosphate. In comparison with the wild-type RT, the Δ69 mutant showed decreased ability to excise primers terminated with AZT monophosphate in the presence of ATP or pyrophosphate (PPi). These data support the role of the excision mechanism in mediating AZT hypersusceptibility. In addition, we demonstrate that the deletion has no effect on resistance to foscarnet (a PPi analogue) on phenotypic and nucleotide incorporation assays carried out with viral clones and recombinant enzymes, respectively. The results of molecular modeling studies suggest that the side chains of Lys65, Asp67, and Lys219 could play an important role in AZT hypersusceptibility mediated by Δ69, whereas in the absence of Thr69, local structural rearrangements affecting the β3–β4 and β11a–β12 loops of the 66-kDa subunit of the RT could reduce the accessibility of the PPi donor to the terminating nucleotide at the 3′ end of the primer.

Keywords: HIV; reverse transcriptase; drug resistance; thymidine analogues; zidovudine

Edited by J. Karn

**Corresponding author.* E-mail address: lmenendez@cbm.uam.es.

Abbreviations used: RT, reverse transcriptase; AZT, β-D-(+)-3′-azido-3′-deoxythymidine; PPi, pyrophosphate; HIV-1, human immunodeficiency virus type 1; MDR, multidrug-resistant; TP, 5′-triphosphate; dNTP, deoxyribonucleoside triphosphate; AZTMP, AZT monophosphate; 3TC, β-L-(−)-2′,3′-dideoxy-3′-thiacytidine; AZTTP, AZT 5′-triphosphate; 3TCTP, 3TC 5′-triphosphate; dTTP, 2′-deoxythymidine 5′-triphosphate; dATP, 2′-deoxyadenosine 5′-triphosphate; dCTP, 2′-deoxycytidine 5′-triphosphate; 3TCMP, 3TC monophosphate; EDTA, ethylenediaminetetraacetic acid.

Introduction

The human immunodeficiency virus type 1 (HIV-1) reverse transcriptase (RT) converts the single-stranded viral genomic RNA into double-stranded DNA that later can be integrated into the host's genome.[1,2] The HIV-1 RT is an asymmetric heterodimer composed of two subunits of 66 and 51 kDa (designated as p66 and p51, respectively). Nucleoside and nonnucleoside RT inhibitors are commonly used in current therapies against HIV infection.[3–6] However, long-term chemotherapy, with repetitive treatment failure and frequent changes in antiretroviral regimens, is often associated with accumulation of drug resistance mutations that confer increased phenotypic resistance and lead to selection of undesirable multidrug-resistant (MDR) HIV-1 strains.

Nucleoside analogues (e.g., zidovudine, lamivudine, stavudine, etc.) are prodrugs that need to be phosphorylated to their active 5′-triphosphate (TP) form in order to compete with their natural deoxyribonucleoside triphosphate (dNTP) counterpart for incorporation into the synthesized DNA. Resistance to nucleoside analogue RT inhibitors is often associated with the appearance of amino acid substitutions at the nucleotide binding site (e.g., K65R, Q151M, M184V, etc.) that reduce the RT's ability to incorporate the triphosphorylated inhibitors.[7–10] An alternative mechanism of resistance to nucleoside RT inhibitors involves the acquisition of mutations such as M41L, D67N, K70R, L210W, T215F/Y, and K219E/Q. Those mutations (commonly designated as thymidine analogue resistance mutations) were shown to increase the ability of RT to excise 3′-terminal chain-terminating inhibitors from blocked DNA primers, through phosphorolysis mediated by ATP or pyrophosphate (PPi).[11,12] This excision activity is most efficient on primers terminated with β-D-(+)-3′-azido-3′-deoxythymidine (AZT, zidovudine) and other thymidine analogues, as well as with tenofovir.[12–15]

Both resistance mechanisms (i.e., nucleotide discrimination and excision of the inhibitor) can be relevant to the acquisition of multidrug resistance.[4] Thus, viral RTs carrying mutations A62V, V75I, F77L, F116Y, and Q151M showed decreased discrimination efficiency against the triphosphorylated forms of zidovudine, didanosine, zalcitabine, stavudine, and abacavir,[8–10] in agreement with high-level resistance to those inhibitors shown by HIV variants that carry those mutations in their RT.[16,17] On the other hand, HIV-1 variants with a dipeptide insertion (usually Ser-Ser, Ser-Gly, or Ser-Ala) between RT codons 69 and 70 in the β3–β4 hairpin loop and additional mutations such as M41L, A62V, K70R, and T215Y showed very high levels of excision activity with primers terminated with AZT monophosphate (AZTMP).[18–20] Dipeptide insertions, as well as deletions in the β3–β4 hairpin loop, are frequently found in heavily mutated MDR HIV-1 isolates from patients who do not respond to the available therapies.[21,22] The prevalence of β3–β4

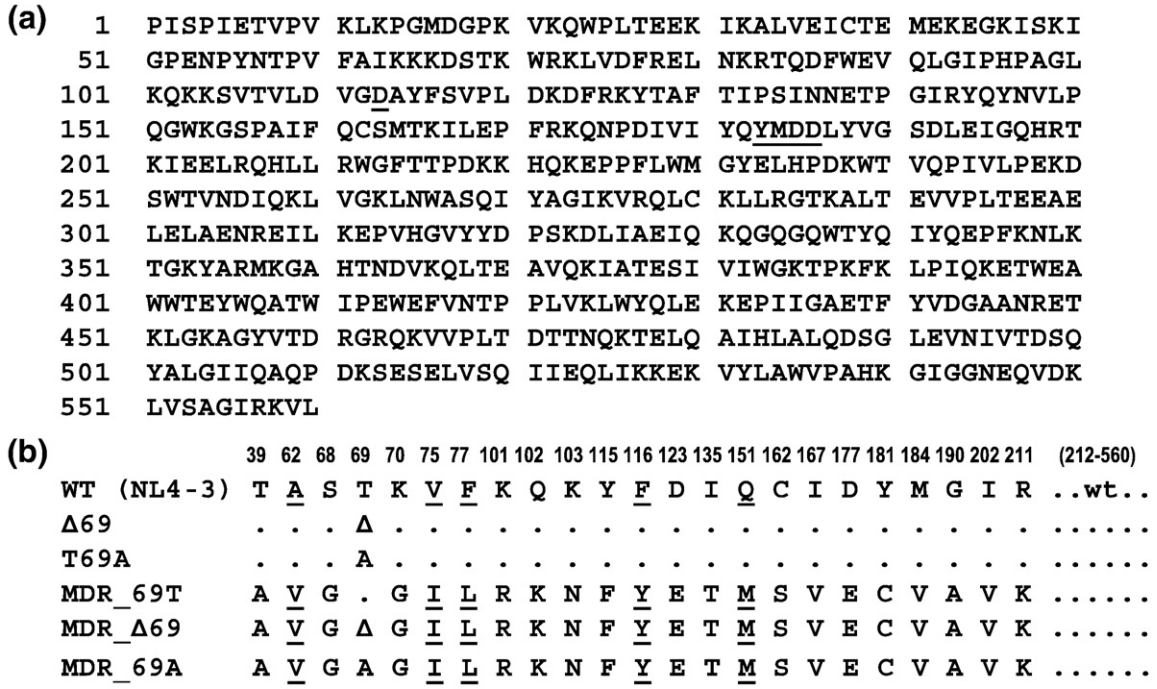

Fig. 1. Amino acid sequences of wild-type and mutant HIV-1 RTs. (a) Amino acid sequence of the wild-type HIV-1 RT (NL4-3 strain). The conserved Asp110 and the YMDD motif are underlined. (b) Sequence differences between the HIV-1_{NL4-3} RT and the mutants analyzed in this study. Residues that are identical with those found in the wild-type enzyme are indicated by dots. Underlined amino acid residues are those characteristic of the Q151M multinucleoside analogue resistance complex.

hairpin loop insertions has been estimated to be around 0.5–2.7%,[23–27] but deletions are less frequently observed, with a prevalence of <0.2% of HIV-infected patients treated with nucleoside RT inhibitors.[28]

A frequent deletion found in viral isolates from treated patients involves the loss of codon 67 in the RT-coding sequence, usually associated with amino acid substitutions T69G and K70R, as well as with one to three thymidine analogue resistance mutations.[28–31] Phenotypic assays revealed that the Δ67 deletion was associated with a large increase in AZT resistance when T69G, K70R, T215F, and K219Q were present.[32] Not surprisingly, the deletion-containing RTs showed high-level excision activity, particularly in the presence of PPi.[33] By itself, the Δ67 deletion conferred low-level phenotypic resistance to lamivudine, zalcitabine, stavudine, and abacavir,[29,30,32,34] but the contribution of the excision and nucleotide discrimination mechanisms to the acquisition of resistance has not been analyzed.

Another one-amino-acid deletion in the β3–β4 hairpin loop of the RT affecting codon 69 (Δ69) appears in viral isolates with RTs containing one or more mutations of the Q151M complex, and sometimes M184V.[34–38] These isolates are usually resistant to multiple nucleoside analogues.[34,38] In the MDR sequence context, the emergence of T69A precedes the appearance of the Δ69 deletion, which improves the replication capacity of the drug-resistant viruses.[38] Interestingly, by itself, Δ69 confers zidovudine hypersusceptibility and low-level resistance to lamivudine and emtricitabine on phenotypic assays.[38]

In this work, we have expressed and purified recombinant RTs containing the Δ69 deletion or the T69A mutation in wild-type and MDR sequence contexts (Fig. 1). Transient kinetics was used to demonstrate that AZT hypersusceptibility cannot be attributed to an effect of the deletion on nucleotide discrimination, but to its effects on ATP- or PPi-mediated excision activity. In contrast, the Δ69 deletion confers low-level resistance to β-L-(−)-2′,3′-dideoxy-3′-thiacytidine (3TC) by reducing the RT's ability to incorporate the inhibitor into the growing DNA chain. In agreement with other studies, we also show that both inhibitors [AZT 5′-triphosphate (AZTTP) and 3TC 5′-triphosphate (3TCTP)] are very poor substrates of MDR variants with the Q151M complex and the M184V mutation, either in the presence or in the absence of the deletion.

Results

Discrimination between 2′-deoxythymidine 5′-triphosphate and AZTTP

Transient kinetic analysis revealed that the wild-type HIV-1_{NL4-3} RT displays a catalytic efficiency (k_{pol}/K_d) of 2′-deoxythymidine 5′-triphosphate (dTTP) incorporation higher that those of its mutant derivatives Δ69 RT and T69A RT (Table 1). These differences are the result of its higher catalytic rate (k_{pol}) and its lower K_d for the incoming nucleotide (Fig. 2a). The higher catalytic efficiency of the wild-type RT was also observed in AZTTP incorporation reactions due to its increased affinity for the triphosphorylated form of the inhibitor. Nevertheless, the discrimination efficiencies against AZTTP were within the range of 1.31–2.13 for the three enzymes (Table 1), suggesting that neither T69A nor the deletion affected nucleotide selectivity in a relevant manner.

The MDR RTs contain several amino acid substitutions that involve residues located at the dNTP binding site (e.g., Y115F, Q151M, M184V, etc.). However, those RTs retained significant DNA polymerase activity. Nucleotide incorporation efficiencies were reduced by less than twofold in comparison with the wild-type enzyme when dTTP was used as substrate (Fig. 2b). In all cases, the observed differences were the result of reduced incorporation rates (k_{pol} values). Unlike for wild-type (NL4-3), Δ69, and T69A RTs, AZTTP was a very poor substrate of RTs containing the MDR complex of mutations, and accurate determination of k_{pol} and K_d was not possible. AZTTP incorporation rates (k_{obs}) in reactions catalyzed by MDR RTs were within the range of 3–6 s^{-1} at the highest nucleotide concentrations tested (typically around

Table 1. Pre-steady-state kinetic constants for the incorporation of dTTP and AZTTP into a heteropolymeric template/primer by wild-type and mutant RTs

Enzyme	Nucleotide	k_{pol} (s^{-1})	K_d (μM)	k_{pol}/K_d (μM^{-1} s^{-1})	Selectivity[a]
Wild type	dTTP	17.4±2.0	7.1±2.5	2.47±0.93	2.13±1.02
	AZTTP	13.4±0.9	2.5±0.7	5.26±1.57	
Δ69	dTTP	12.3±1.0	14.8±3.0	0.83±0.18	2.02±0.61
	AZTTP	16.7±1.1	9.9±2.0	1.68±0.35	
T69A	dTTP	14.2±1.8	10.1±4.1	1.41±0.60	1.31±0.58
	AZTTP	15.8±0.6	8.5±1.1	1.85±0.24	
MDR_69T	dTTP	7.4±0.4	5.9±1.7	1.25±0.37	
MDR_Δ69	dTTP	8.2±0.3	4.9±0.8	1.65±0.27	
MDR_69A	dTTP	10.5±0.9	9.4±2.7	1.11±0.33	

The template/primer 31T/21P was used as substrate. Data shown are the mean±SD of a representative experiment. Each of the assays was performed independently at least twice. Interassay variability was below 20%.

[a] Selectivity is the ratio of k_{pol}/K_d (AZTTP) to k_{pol}/K_d (dTTP).

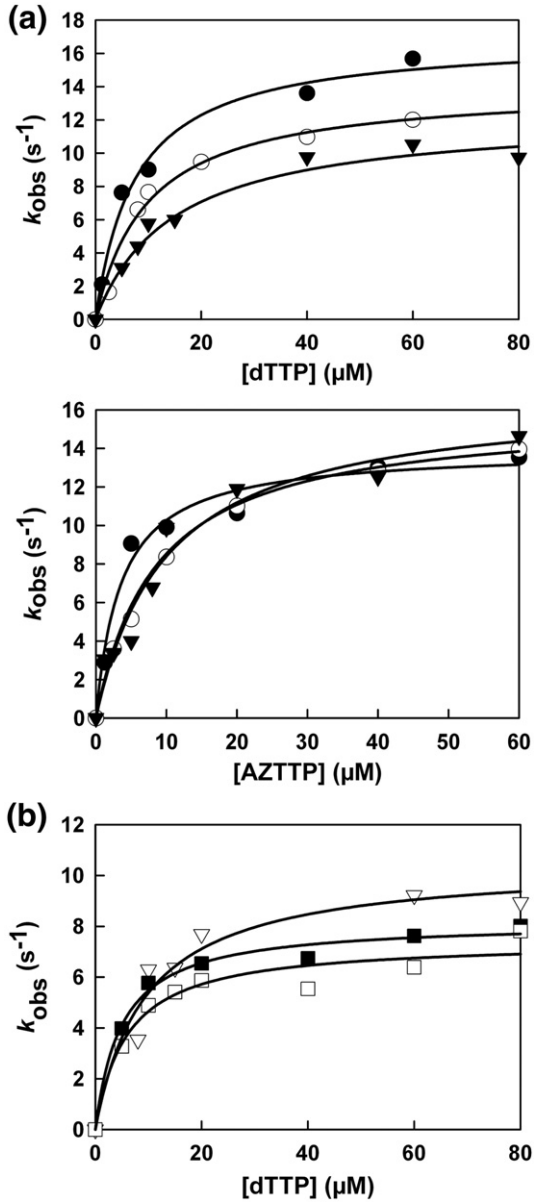

Fig. 2. Nucleotide concentration dependence on the first-order rates for dTTP and AZTTP incorporation into DNA/DNA 31/21-mer. (a) Rates of DNA-dependent incorporation by wild-type HIV-1 RT (●) and mutants Δ69 (▼) and T69A (○) in the presence of varying concentrations of dTTP or AZTTP. (b) Concentration dependence of dTTP incorporation into the 31T/21P template/primer by mutant RTs MDR_69T (□), MDR_Δ69 (■), and MDR_69A (▽). Incorporation rates (k_{obs}) from the corresponding burst or single-exponential equations (not shown) were plotted against the nucleotide concentrations, and the data were fitted to the hyperbolic equation to obtain K_d and k_{pol} values.

100 μM), but in all cases, K_d values were estimated to be well above 40 μM (data not shown).

These results indicate that the phenotypic resistance to AZT observed with a virus containing the MDR variants could be attributed to their reduced ability to incorporate the inhibitor. The effects on AZTTP incorporation of T69A or the Δ69 deletion in the MDR sequence context were assessed under steady-state conditions (Table 2). However, we did not detect large differences in the k_{cat} and K_m values obtained with the three RTs, although a slightly higher catalytic efficiency (k_{cat}/K_m) was observed with the MDR_Δ69 RT.

Excision of AZTMP from blocked DNA primers and phenotypic susceptibility to AZT and foscarnet

The ability of RTs to rescue AZTMP-terminated primers was assessed by using the template/primer shown in Fig. 3. These experiments were carried out in two steps. First, the enzyme and the template/primer were incubated in the presence of AZTTP to generate a terminated 26-nucleotide primer. Then, unblocking and extension reactions were carried out by adding a mixture of dNTPs and a PPi donor. In the presence of 3.2 mM ATP, wild-type and mutant Δ69 and T69A RTs showed low excision activity. However, the ATP-dependent phosphorolytic activity of the Δ69 mutant was reduced by twofold in comparison with the other two RTs that showed similar levels of excision activity (Fig. 3).

The effects of the deletion on the RT's phosphorolytic activity were further demonstrated in the presence of PPi. In the presence of either 20 or 200 μM PPi, the RT carrying the deletion showed reduced PPi-dependent phosphorolytic activity with primers terminated with AZTMP (Fig. 4). These differences were consistently observed within a wide range of PPi concentrations. The rate of pyrophosphorolytic removal of AZTMP was reduced by twofold in the deletion mutant, in comparison with the wild-type enzyme and the T69A RT. As expected, MDR RTs had very low phosphorolytic activities (data not shown), in agreement with their decreased ability to incorporate the inhibitor.

Rescue reactions were inhibited by the next complementary dNTP [2′-deoxyadenosine 5′-triphosphate (dATP) under our assay conditions]. Differences between the three enzymes tested were relatively small, although Δ69 was less susceptible to dNTP inhibition than the other two enzymes (Fig. 5).

Phenotypic data showing the AZT hypersusceptibility of a recombinant virus containing a three-nucleotide deletion at codon 69 of the RT-coding region were consistent with the reduced excision activity, shown in assays with the Δ69 RT (Table 3). HIV-1 variants harboring the Δ69 deletion showed about a sixfold increased susceptibility to AZT. Although AZT hypersusceptibility appears to be a consequence of reduced pyrophosphorolytic activity, foscarnet inhibition was not affected by changes affecting position 69. Interestingly, the MDR_Δ69 RT retained susceptibility to foscarnet on phenotypic assays (Table 3). These results were consistent with the foscarnet susceptibility data calculated for dTTP incorporation assays carried out with the recombinant enzymes. In those assays, the foscarnet IC_{50} values were 110.7±32.5 μM for wild-type RT, 93.7±

Table 2. Steady-state kinetic constants for the incorporation of dTTP and AZTTP into a heteropolymeric template/primer by wild-type and MDR RTs

Enzyme	Nucleotide	k_{cat} (min^{-1})	K_m (μM)	k_{cat}/K_m (μM^{-1} min^{-1})
Wild type	dTTP	2.30±0.09	0.129±0.017	17.83±2.45
	AZTTP	1.32±0.09	0.048±0.012	27.50±7.12
MDR_69T	AZTTP	2.19±0.10	17.2±3.8	0.13±0.03
MDR_Δ69	AZTTP	1.65±0.13	6.7±2.1	0.25±0.08
MDR_69A	AZTTP	2.12±0.09	11.0±1.9	0.19±0.03

After formation of the RT–DNA/DNA complex, 31T/21P elongation reactions were incubated at 37 °C for 10, 20, 30, and 40 s to determine the rate of product formation in steady state at each nucleotide concentration. Data are presented as mean±SD, obtained from a nonlinear least-squares fit of the kinetics data of a representative experiment to the Michaelis–Menten equation. Each of the assays was performed independently at least three times. Interassay variability was below 20%.

20.6 μM for Δ69 RT, 307.5±119.5 μM for T69A RT, and 48.3±12.6 μM for the MDR_Δ69 RT.

Discrimination between 2′-deoxycytidine 5′-triphosphate and 3TCTP

Transient kinetic analysis showed that the catalytic efficiency (k_{pol}/K_d) of 3TCTP incorporation by wild-type RT was largely reduced in comparison with 2′-deoxycytidine 5′-triphosphate (dCTP) incorporation (Table 4). The reduced catalytic efficiency of 3TCTP incorporation resulted from an 8-fold increase in K_d and a 175-fold decrease in k_{pol}. The kinetic parameters for the incorporation of dCTP were similar for all of the three enzymes tested (Fig. 6a), although the Δ69 mutant RT showed a higher catalytic efficiency due to its lower K_d for dCTP. Interestingly, the Δ69 mutant showed a 3-fold reduction in the catalytic efficiency of 3TCTP incorporation, in comparison with the wild-type and T69A RTs (Fig. 6b). The combined effects of increased dCTP incorporation and decreased 3TCTP incorporation by Δ69 RT resulted in a 6-fold reduction in the enzyme's ability to discriminate between dCTP and 3TCTP, consistent with the increased lamivudine resistance observed on phenotypic assays with recombinant HIV-1 clones containing the deletion of codon 69 in the viral RT.[38] Incorporation of 3TCTP by MDR RTs was negligible even at high concentrations of the inhibitor (i.e., 100 μM) due to the presence of M184V in their amino acid sequence (Fig. 1); therefore, the effects of the deletion in the MDR sequence context were not evaluated.

Excision of 3TC monophosphate from blocked DNA primers

The ATP- or PPi-dependent phosphorolytic activity of excision-proficient RTs was very low when assessed with primers terminated with 3TC monophosphate (3TCMP).[15] By increasing the RT concentration relative to the template/primer concentration, we were able to detect 3TCMP excision in the pre-

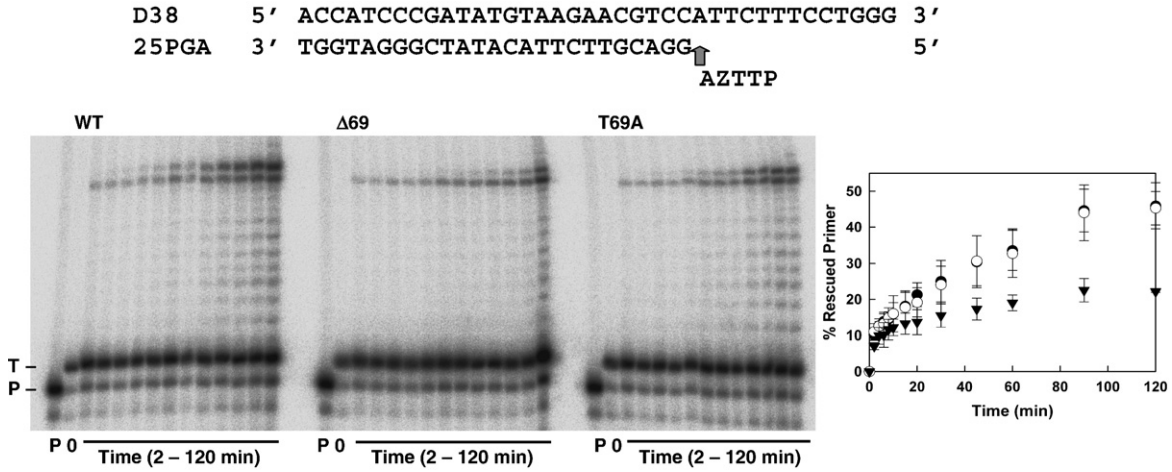

Fig. 3. ATP-dependent excision efficiencies of wild-type and mutant RTs with primers terminated with AZTMP. Rescue DNA polymerization reactions were carried out with a heteropolymeric template/primer whose sequence is given above. First, AZTTP was incorporated at position +1 of the 25-nucleotide primer (P) (lane P) to generate a 26-nucleotide product (T) (lane 0). Excision of AZTMP and further extension of the primer in the presence of ATP (3.2 mM) and a mixture of dNTPs containing 100 μM dCTP, deoxyguanosine triphosphate, and dTTP, and 1 μM dATP. Aliquots are removed 2, 4, 6, 8, 10, 15, 20, 30, 45, 60, 90, and 120 min after addition of ATP. Time courses of primer rescue reactions catalyzed by wild-type HIV-1 RT (●) and mutants Δ69 (▼) and T69A (○) are shown on the right. The template/primer and active enzyme concentrations in these assays were 25 and 60 nM, respectively. Represented values were obtained from three independent experiments. Interassay variability was below 20% in these experiments.

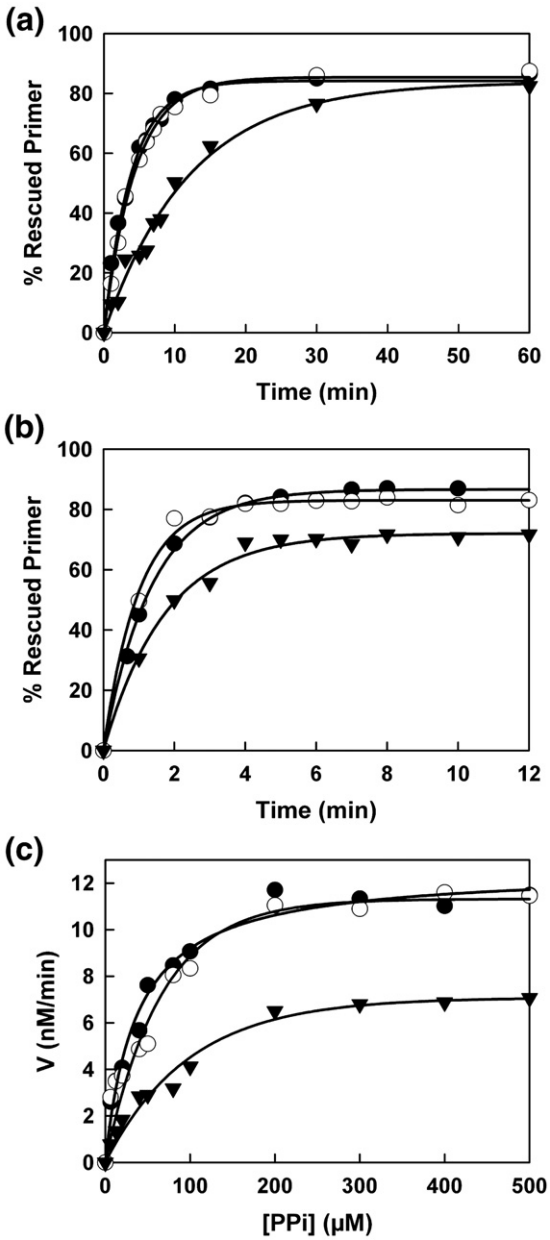

Fig. 4. Effect of mutations on PPi-dependent excision efficiencies with primers terminated with AZTMP. Time courses of primer rescue reactions catalyzed by wild-type HIV-1 RT (●) and mutants Δ69 (▼) and T69A (○) were carried out in the presence of 20 μM PPi (a) and 200 μM PPi (b). The assays were performed with the template/primer D38/25PGA at 30 nM. All of the dNTPs were supplied at 100 μM, except for dATP, whose concentration was 1 μM. Active enzyme concentration in these assays was 20 nM. Represented values were obtained from two to three independent experiments. Standard deviations were <20% in these assays. (c) Dependence of the excision rate for AZTMP removal on PPi concentration for wild-type HIV-1 RT (●) and mutants Δ69 (▼) and T69A (○).

sence of 200 μM PPi, while at lower concentrations (i.e., 20 μM PPi), the efficiency of the excision reaction was very low (Fig. 7a). Δ69 RT showed the lowest excision activity in the presence of 200 μM PPi. In the presence of 3.2 mM ATP, the excision activities of

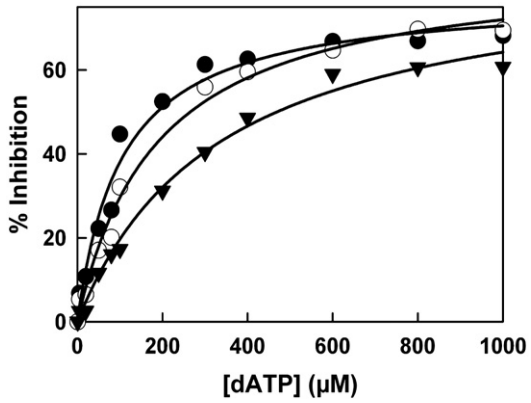

Fig. 5. Ability of the next complementary dNTP to inhibit the excision reaction with primers terminated with AZTMP in the presence of PPi. Assays were carried out in the presence of 200 μM PPi. All dNTPs in these assays were supplied at 100 μM, except for dATP, whose concentration ranged from 1 to 1000 μM, depending on the assay. Active enzyme concentration in the assay was 20 nM, and the concentration of the template/primer D38/25PGA was 30 nM. Samples were incubated for 0–5 min, depending on the assay. In all cases, incubation times were within the linear range of the corresponding time course. Percent inhibition was plotted against the concentration of dATP, and the data were fitted to a hyperbola to obtain the IC_{50} for each enzyme: 119.7±36.1 μM for wild-type HIV-1 RT (●), 336.2±40.4 μM for mutant Δ69 (▼), and 188.7±24.5 μM for mutant T69A (○). Interassay variability was below 20% in these experiments.

wild-type and Δ69 RTs were very low (Fig. 7b). Overall, these effects contribute to the higher lamivudine resistance observed on phenotypic assays with the HIV-1 variant containing the Δ69 RT.

Structural model for the ternary complex of Δ69 RT, double-stranded DNA, and dTTP

The first structural model, based on 1RTD coordinates, was refined by molecular dynamics. Simulations were followed over the 10-ns trajectory. In comparison with the reported crystal structure for the ternary complex containing the wild-type RT,[39] the root mean square deviation(s) (rmsd) corresponding to the backbone C^{α} atoms of the modeled ternary complex remained below 2.2 Å during all

Table 3. Susceptibility of HIV-1 constructs to AZT and foscarnet

	IC_{50} (μg/ml)	
RTs	AZT	Foscarnet
Wild type	$(1.6\pm0.9)\times10^{-3}$	8.8±1.7
Δ69	$(2.6\pm1.5)\times10^{-4}$ (0.16×)	8.1±1.3 (0.9×)
T69A	$(9.0\pm1.0)\times10^{-4}$ (0.6×)	10.9±1.4 (1.2×)
MDR_Δ69	>1 (>1000×)	4.6±1.8 (0.5×)

The IC_{50} values represent the mean±SD of three tests, with each one performed six times. The fold increase in IC_{50} relative to the wild-type HXB2 virus control carrying the RT sequence of NL4-3 is shown in parentheses.

Table 4. Pre-steady-state kinetic constants for the incorporation of dCTP and 3TCTP into a heteropolymeric template/primer by wild-type and mutant RTs

Enzyme	Nucleotide	k_{pol} (s^{-1})	K_d (μM)	k_{pol}/K_d ($\mu M^{-1}\ s^{-1}$)	Selectivity[a]
Wild type	dCTP	9.8±0.4	3.7±0.7	2.66±0.51	$(7.2\pm2.1)\times10^{-4}$
	3TCTP	0.056±0.005	29.2±5.7	$(1.92\pm0.41)\times10^{-3}$	
Δ69	dCTP	8.5±0.5	1.6±0.5	5.41±1.75	$(1.09\pm0.39)\times10^{-4}$
	3TCTP	0.022±0.001	37.4±5.8	$(5.88\pm0.96)\times10^{-4}$	
T69A	dCTP	10.6±0.8	4.3±1.6	2.49±0.97	$(7.1\pm3.6)\times10^{-4}$
	3TCTP	0.045±0.006	25.4±7.4	$(1.77\pm0.57)\times10^{-3}$	

The template/primer 31G/21P was used as substrate. Data shown are the mean±SD of a representative experiment. Each of the assays was performed independently at least twice. Interassay variability was below 20%.

[a] Selectivity is the ratio of k_{pol}/K_d (3TCTP) to k_{pol}/K_d (dCTP).

simulation times (<1.7 Å when the β3–β4 hairpin loop and residues 214–228 were not included in the comparison) (Fig. 8a). At the end of the simulation, interactions at the catalytic site of the ternary complex containing the Δ69 RT (including the octahedral coordination shells of the catalytic Mg^{2+}) were close to those observed in the crystal structure (Table 5), and the catalytic attack distance was reduced to approximately 3 Å within the first 0.4 ns of the simulation (Fig. 8b).

The largest differences between the modeled structure of Δ69 RT and the crystal structure of wild-type HIV-1 RT were observed at the β3–β4 hairpin loop (residues 63–73) and between β-strand 11a (residues 214–217) and β-strand 12 (residues 227–229). According to the model, the loss of Thr69 leads to the extension of β-strands 3 and 4, which may increase the stability of the loop while reducing its conformational flexibility (Fig. 9). Simultaneously, the polypeptide backbone within residues 217 and 227 moves towards the dNTP binding site, allowing the interaction of the side chain of Lys219 with the nonbridging oxygen atoms of the γ-phosphate of the incoming dNTP. The Asp67-Lys219 salt bridge observed in the crystal structure is lost in the Δ69 RT model, while the side chain of Asp67 could now interfere with the interaction of Lys65 with the incoming dNTP.

Discussion

The β3–β4 hairpin loop of HIV-1 RT includes residues 63–73 and plays an important role in the stabilization of the dNTP/Mg^{2+} complex within the nucleotide binding site of the polymerase, mainly through the establishment of hydrogen bonds between the side chains of Lys65 and Arg72 and nonbridging oxygen atoms in the TP moiety of the dNTP.[39] It has been demonstrated that the formation of a catalytically competent DNA polymerase complex is triggered by binding of free Mg^{2+};[40] when this occurs, the hairpin loop undergoes significant rearrangements of its side chains, as revealed by molecular dynamics simulations.[40] Not surprisingly, insertions and deletions in the β3–β4 hairpin loop of the RT may appear in drug-resistant isolates, usually in combination with amino acid substitutions related to drug resistance.

Two distinct patterns of drug resistance mutations have been observed in clinical isolates containing a deletion of one amino acid in the β3–β4 loop of the viral RT. Thymidine analogue resistance mutations such as K70R or T215F/Y appear associated with the deletion of Asp67, while Q151M and other mutations of the Q151M complex (i.e., A62V, V75I, F77L, and F116Y) are usually found in combination with the deletion of Thr69. On phenotypic assays, MDR isolates containing the Q151M complex of mutations and the amino acid substitutions K103N, Y115F, Y181C, M184V, and G190A showed high-level resistance to nucleoside analogues both in the presence and in the absence of the deletion.[38] Our results show that AZTTP and 3TCTP are poor substrates of the MDR RTs. In the case of 3TCTP, the presence of M184V is the likely cause of their resistance to the inhibitor.[7] However, in the case of AZTTP, resistance could be attributed to the presence of the five mutations forming the Q151M complex.[8] It has been noted that, under similar assay conditions, the incorporation of AZTTP by mutant RTs bearing A62V/V75I/F77L/F116Y/Q151M proceeded at a rate constant (k_{pol}) that was about seven times lower than the k_{pol} for the incorporation of dTTP.[8] This k_{pol} effect was not observed with the wild-type RT. However, the AZTTP resistance shown by MDR RTs used in this work was largely attributed to a K_d effect, suggesting that other mutations affecting nucleotide-binding residues (i.e., Y115F, M184V, and substitutions at the β3–β4 hairpin loop) may contribute to their decreased ability to use AZTTP as a DNA polymerization substrate.

Extensive analysis of the effects of the deletion on inhibitor specificity was not possible due to the intrinsic resistance of the mutant MDR RTs. However, our data showed no effects of the deletion on drug resistance, in agreement with our previously published phenotypic data.[38] Interestingly, catalytic efficiencies of dCTP and dTTP incorporation by MDR_Δ69 RT were somewhat higher than for MDR_69A and MDR_69T RTs, in agreement with fitness data showing that the deletion increased the replication capacity of the virus containing the mutational pattern of the MDR variants. Although these data could explain why Δ69 is selected in a virus having the MDR complex of mutations and why these variants outcompete those containing T69A, other factors, including RT heterodimer

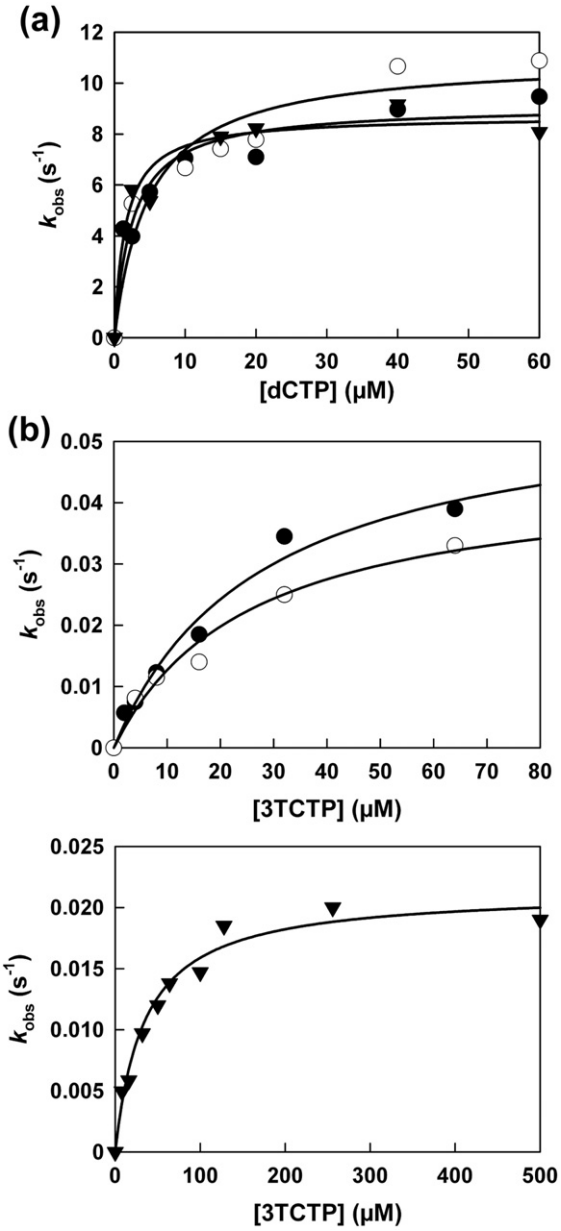

Fig. 6. Nucleotide concentration dependence on the first-order rates for dCTP and 3TCTP incorporation into DNA/DNA 31/21-mer. Rates of DNA-dependent incorporation by wild-type HIV-1 RT (●) and mutants Δ69 (▼) and T69A (○) in the presence of varying concentrations of dCTP and 3TCTP are shown in (a) and (b), respectively. Incorporation rates (k_{obs}) from the corresponding burst or single-exponential equations (not shown) were plotted against the nucleotide concentrations, and the data were fitted to the hyperbolic equation to obtain K_d and k_{pol} values.

stability, could be responsible for the increased fitness of the Δ69-containing variants.[38,41]

The deletion of codon 69 of the RT-coding region is most frequent in isolates containing multiple resistance mutations, including Q151M. However, there are examples of Δ69 appearing early under antiretroviral drug pressure. Thus, Δ69 has been found either in combination with V75I/V and F77L/F or with K65R, K103N, and Y181C in isolates from HIV-infected patients treated with didanosine and stavudine who had been previously exposed to lamivudine and other RT inhibitors,[35,42] or in combination with K65R, K70R, and V106M in individuals treated with lamivudine, stavudine, and efavirenz.[43] Despite the common occurrence of lamivudine in regimens preceding the emergence of the deletion, Δ69 (together with K70R) has also been found in the absence of other relevant drug resistance mutations in untreated patients.[44]

The molecular model of Δ69 RT, in complex with DNA and an incoming dNTP, indicates that the deletion of Thr69 does not affect critical interactions required for maintaining the catalytic attack distance between the 3′-OH of the primer and α-phosphorus, and is consistent with the high catalytic efficiency of nucleotide incorporation of the Δ69 RT mutant. According to the model, we predict that the interaction of the side chain of Lys65 with the incoming dNTP could be substituted with an equivalent interaction with the side chain of Lys219. A role in nucleoside analogue resistance has been proposed for the potential interchange of Lys65 and Lys219 contacts with the γ-phosphate, based on the analysis of the crystal of ternary complexes of HIV-1 RT containing tenofovir diphosphate.[45] The loss of the interaction of Lys65 suggested in our model would also explain why K219E or K219Q (two typical thymidine analogue resistance mutations) is rarely associated with the deletion of Thr69.

The introduction of Δ69 in the context of a wild-type sequence renders an HIV-1 variant with 3.5- to 5-fold increased resistance to lamivudine and emtricitabine on phenotypic assays.[38] Transient kinetic data reported in this study show that lamivudine resistance mediated by Δ69 results from the decreased efficiency of 3TCTP incorporation relative to dCTP incorporation in comparison with the wild-type enzyme. As reported in Table 4, the efficiency of incorporation of 3TCTP by the wild-type RT is reduced by about 3 orders of magnitude in comparison with dCTP incorporation in DNA-dependent DNA polymerase reactions. As reported for other lamivudine-resistant RTs, the differences were the result of a large reduction in the catalytic rate constant (k_{pol}) of the inhibitor.[46–48] Thus, Δ69 increases the catalytic efficiency of dCTP incorporation, while 3TCTP incorporation efficiency decreases in comparison with the wild-type RT. These effects result from the combination of a reduction in the catalytic rate constant and a loss of affinity for the inhibitor—an effect that has been previously reported for RTs containing the drug resistance mutation M184V.[9] Excision of 3TCMP by all of the tested mutants was negligible under our assay conditions, in agreement with published results obtained with other RTs.[15,49] In comparison with the wild-type RT, Δ69 showed decreased PPi-mediated excision activity on 3TCMP-terminated primers (Fig. 7), an effect that has been also reported for

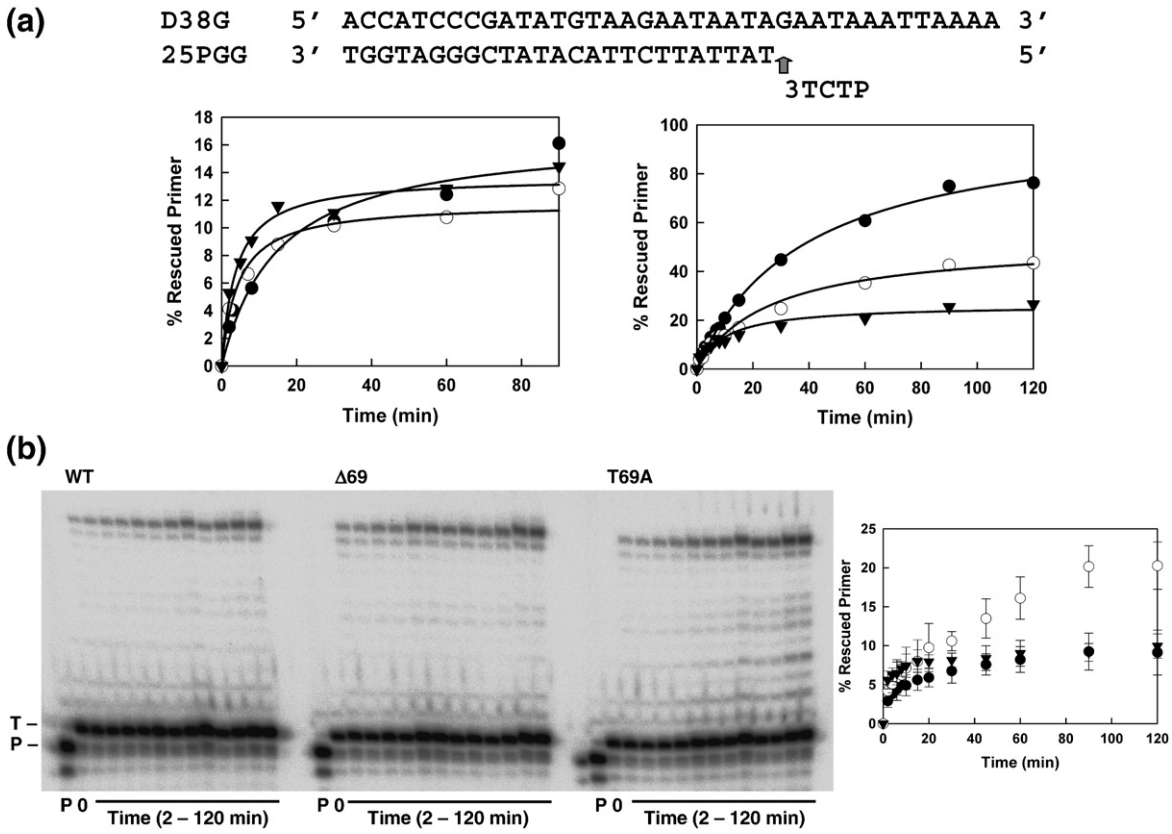

Fig. 7. Effect of mutations on rescue DNA polymerization reactions initiated from primers terminated with 3TCMP. (a) Time courses of the excision reactions carried out in the presence of 20 μM PPi (left) and 200 μM (right) and catalyzed by wild-type HIV-1 RT (●) and mutants Δ69 (▼) and T69A (○). (b) Gels showing excision reactions carried out with wild-type HIV-1 RT (●) and mutants Δ69 (▼) and T69A (○) in the presence of 3.2 mM ATP. Samples loaded into the gel correspond to the unextended primer and to aliquots removed 2, 4, 6, 8, 10, 15, 20, 30, 45, 60, 90, and 120 min after the addition of ATP and a mixture of dNTPs at a final concentration of 100 μM (except for dATP, which was supplied at 1 μM). Time courses of the rescue reactions catalyzed by wild-type RT (●) and mutants Δ69 (▼) and T69A (○) are shown on the right. All assays were performed with template/primer D38G/25PGG (shown above) at 25 nM and using active RT concentrations of 20 nM (for excision reactions catalyzed in the presence of PPi) and 60 nM (for excision reactions carried out with ATP). The concentration of 3TCTP in the blocking reaction was 200 μM. Represented values were obtained from three independent experiments. Interassay variability was below 20% in these experiments.

the M184V mutation.[50] In those studies, it was also shown that M184V compromised the ATP- and PPi-mediated excision of primers terminated with AZTMP.[50]

By itself, Δ69 confers fivefold increased susceptibility to AZT on phenotypic assays.[38] Our mechanistic studies reveal that these differences cannot be attributed to impaired discrimination ability between AZTTP and dTTP, but to the lower ATP- and PPi-dependent phosphorolytic activity of the deletion-containing RT. Our results show that the Δ69 RT excises AZTMP from blocked primers at a rate lower than those in the wild-type enzyme and the mutant T69A RT over a wide range of PPi concentrations (6–500 μM), suggesting that AZT hypersusceptibility could be observed not only in replicating cultures (e.g., MT-4 cells) but also in macrophages and unstimulated $CD4^+$ or $CD8^+$ T cells where the PPi concentration was estimated at 7–15 μM.[51] Both wild-type and Δ69 RTs showed very low levels of ATP-dependent phosphorolytic activity in the presence of 3.2 mM ATP.

It has been shown that several mutations conferring resistance to foscarnet (a PPi analogue) increase viral susceptibility to AZT (i.e., K65R, W88G, E89K, etc.), particularly in the presence of thymidine analogue resistance mutations such as D67N, K70R, T215Y, and K219Q.[52] However, Δ69 does not have an effect on foscarnet susceptibility neither in polymerization reactions carried out with the recombinant enzyme nor in phenotypic assays using recombinant HIV-1 strains bearing the deletion.

Interestingly, at very high concentrations (>2.5 mM), foscarnet is able to remove AZTMP from blocked DNA primers, albeit very inefficiently.[53] Under our assay conditions, foscarnet-mediated excision rates (k_{rem}) were found to be very low (~0.004 min^{-1}) and similar for wild-type RT and mutants T69A and Δ69 (data not shown). In comparison with PPi, foscarnet has a smaller volume; therefore, steric effects affecting its interaction with the side chains of Lys65 and Lys219 would be reduced. The deletion of Thr69 impairs excision, probably by altering interactions with the phosphate group of the PPi

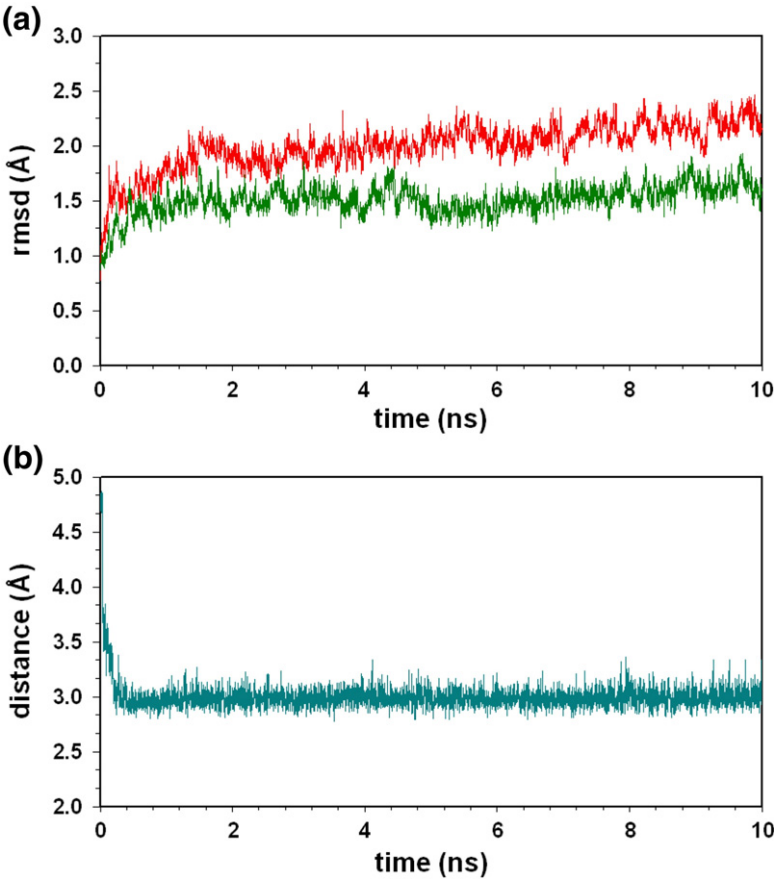

Fig. 8. Conformational changes in the Δ69 HIV-1 RT ternary complex occurring along the simulation time. (a) Evolution of the rmsd of the C^{α} atoms of the polymerase domain of the 66-kDa subunit of the RT (fingers, palm, and thumb subdomains), excluding residues 63–73 and 214–228 (green), and the whole polymerase domain (residues 1–379) (red). (b) Evolution of the interatomic distance between 3′O of the primer and the α-phosphorus of the incoming dTTP during molecular dynamics simulation.

donor that locates at a position distal to the 3′ end of the primer. Local structural rearrangements, including the conformational changes predicted by molecular dynamics and affecting the β3–β4 and β11a–β12 loops, could also reduce the accessibility of the PPi donor to the terminating nucleotide at the 3′ end of the primer. Modeling studies lead us to hypothesize that the interactions involving the side chains of Asp67 and Lys219 could play an important role in AZT hypersusceptibility mediated by Δ69. Studies addressing whether thymidine analogue resistance mutations D67N and K219E/Q could affect AZT susceptibility when the deletion is present are currently in progress and should help us to decipher the role of specific residues involved in the excision reactions, as well as relevant interactions for the phosphorolytic activity that mediates resistance to nucleoside analogue RT inhibitors.

Table 5. Active site interatomic distances (in Å) for the simulated Δ69 HIV-1 RT ternary complexes and the crystal form (1RTD)

Distance	1RTD (X-ray)	Δ69 RT/DNA/dTTP/2Mg^{2+} (10 ns)
Mg^{2+} (A)–Asp110:OD2	2.60	1.87
Mg^{2+} (A)–Asp185:OD1	2.12	1.86
Mg^{2+} (A)–Asp186:OD2	3.65	1.94
Mg^{2+} (A)–dTTP:O1A	3.02	2.06
Mg^{2+} (A)–A primer:O3′	NA	2.05
Mg^{2+} (A)–water:OH	NA	1.96
Mg^{2+} (B)–Asp110:OD1	2.12	1.90
Mg^{2+} (B)–Val111:O	2.23	2.09
Mg^{2+} (B)–Asp185:OD2	2.31	1.91
Mg^{2+} (B)–dTTP:O1A	2.20	1.95
Mg^{2+} (B)–dTTP:O2B	2.43	1.84
Mg^{2+} (B)–dTTP:O1G	2.39	1.86
A primer:O3′–dTTP:Pα	NA	3.10

NA, not available.

Materials and Methods

Mutagenesis, expression, and purification of recombinant RTs

The three-nucleotide deletion found at codon 69 in the RT-coding region of HIV-1_{MDRc7b},[38] which contains the MDR_Δ69 RT (Fig. 1), was eliminated by inserting a triplet encoding for the wild-type Thr (MDR_69T) using the GeneTailor™ Site-Directed Mutagenesis System (Invitrogen). Mutagenesis reactions were carried out by following the manufacturer's instructions, using plasmid pJM14 (MDR_Δ69) as template DNA and the mutagenic primers 5′-AGAAAAAAGACGGTACTGGATGGAGAAAAT-3′ and 5′-ACCGTCTTTTTTCTTTATGACGAAGACTG-GAG-3′. Derivatives of pJM14 containing the wild-type HIV-1_{NL4-3} RT and mutants T69A and Δ69, as well as the MDR_69A RT (HIV-1_{MDRc3b}), were available from previous studies.[38]

The wild-type RT and mutants T69A and Δ69 were amplified by PCR with primers 5′-GCACTTTCAATTGT-CCCATTAGTCCTATTGAGAC-3′ (NMF) and 5′-CCATC-

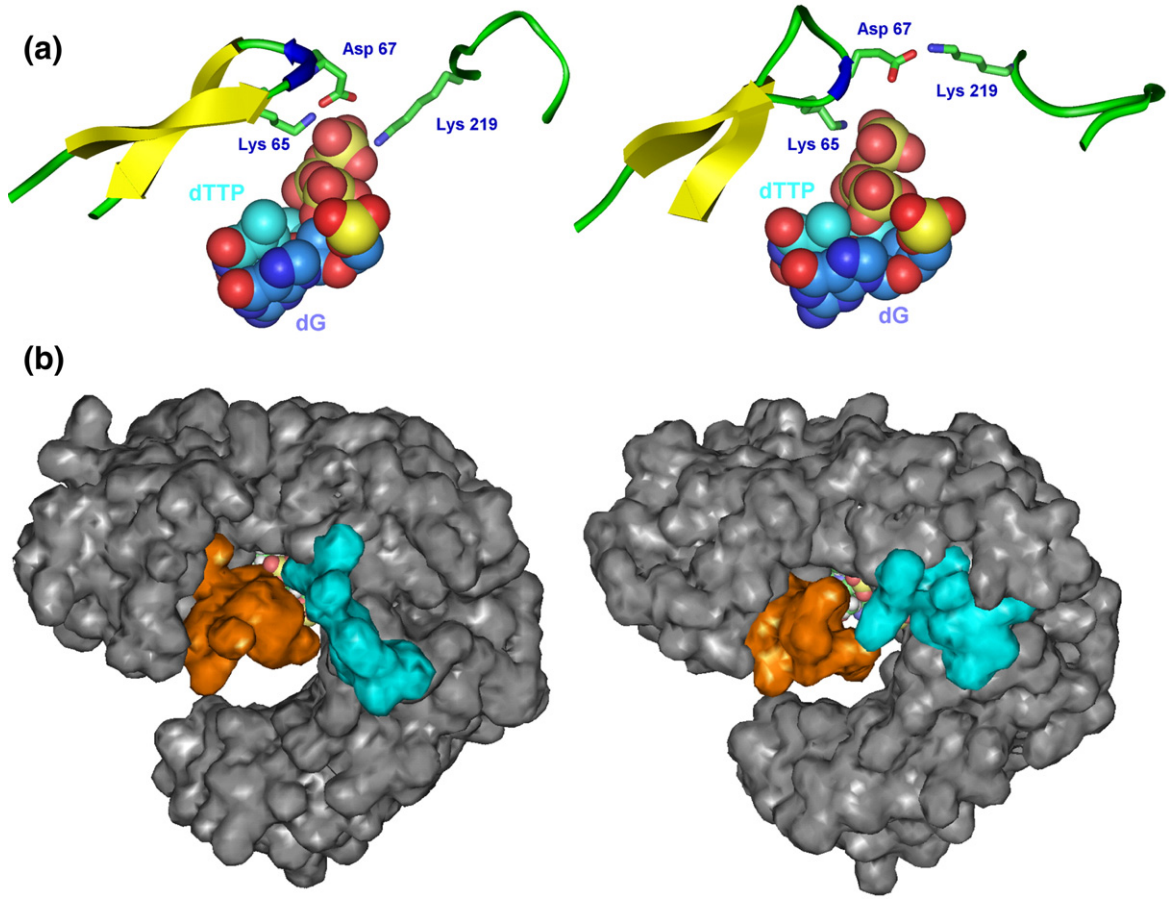

Fig. 9. Comparison of the structural model of mutant Δ69 and the crystal structure of wild-type HIV-1 RT. (a) Ribbon representation of the polypeptide backbone of residues 63–73 and 214–228 in the Δ69 RT modeled structure (left) and in the crystal structure of the ternary complex containing wild-type HIV-1 RT, a DNA–DNA template/primer, and an incoming dNTP (right). The side chains of Lys65, Arg67, and Lys219 are shown with a stick representation. The incoming nucleotide (dTTP) and the nucleotide at the 3′ end of the primer are represented with a CPK model. (b) View of the surface of the molecular model of Δ69 RT (left) and the crystal structure of the wild-type RT (right) showing the location of β3–β4 hairpin residues 63–73 (orange) and residues 214–228 (green). The incoming dNTP (partially hidden by the colored structures) is represented with a CPK model. Wild-type HIV-1 RT sequence numbering is used in both panels.

TAACTCGAGTACTTTCCTGATTCC-3′ (CXH), while MDR_69T, MDR_69A, and MDR_Δ69 were amplified with primers 5′-GCACTTTGAATTCTCCCATTAGTCC-TATTGAGAC-3′ (NEC) and CXH. PCR amplifications were performed in 20 mM Tris–HCl (pH 8.8), 10 mM KCl, 10 mM $(NH_4)_2SO_4$, 2 mM $MgSO_4$, 0.1% Triton X-100, 0.1 mg/ml bovine serum albumin, 50 μM of each of the four dNTPs, 200 ng of each primer, 1 μg of template DNA, and 1.5 U of Pfu DNA polymerase (Promega). The amplification reactions were initiated with incubation at 95 °C for 2 min, followed by 20 cycles of 95 °C for 30 s, 55 °C for 1 min, and 68 °C for 4 min, and final incubation at 68 °C for 5 min. The purified DNA obtained from the PCR was cleaved with MfeI and XhoI (amplifications of wild-type NL4-3 RT and mutants T69A and Δ69), or with EcoRI and XhoI (MDR variants), and cloned into the expression vector pRT66B(BH10).[54] All constructs were verified by restriction enzyme analysis and nucleotide sequencing.

Recombinant heterodimeric RTs were expressed and purified as previously described.[54,55] Thus, RT p66 subunits carrying a His_6 tag at their C-terminus were coexpressed with HIV-1 protease in *Escherichia coli* XL1 Blue to obtain p66/p51 heterodimers, which were later purified by ionic exchange, followed by affinity chromatography. Enzymes were quantified by active-site titration[56] before biochemical studies.

Nucleotides and template/primers

Stock solutions (100 mM) of dNTPs and rNTPs, and [γ-^{32}P]ATP were obtained from GE Healthcare. The TP derivatives of NRTIs were obtained from Trilink BioTechnologies (AZTTP) and Sierra Bioresearch (3TCTP). Before use, nucleoside TPs were treated with inorganic pyrophosphatase to remove traces of PPi, as described.[15] DNA oligonucleotides 21P (3′-CCTATGTATACCAATTTCATA-5′), 31T (3′-TATGAAATTGGTATACATAGGATTTTTTTTT-5′), 31C (3′-TATGAAATTGGTATACATAGGGTTTTTTTT-5′), 25PGA (3′-GGACGTTCTTACATATCGGGATGGT-5′), 25PGG (3′-TATTATTCTTACATATCGGGATGGT-5′), D38 (3′-ACCATCCCGATATGTAAGAACGTCCATTCTTTC-CTGGG-5′), and D38G (3′-ACCATCCCGATATGTAAGA-ATAATAGAATAAATTAAAA-5′) were obtained from Life Technologies. Oligonucleotides 21P, 25PGA, and 25PGG were labeled at their 5′ termini with [γ-^{32}P]ATP and T4 polynucleotide kinase, and then annealed to their corresponding templates (31T or 31C, D38, and D38G, respec-

tively). Template/primers 31T/21P and 31C/21P were used in transient kinetics experiments, while D38/25PGA and D38G/25PGG were used in excision reactions.

Pre-steady-state kinetic assays

Transient kinetic parameters for nucleotide incorporation by wild-type and mutant RTs were determined with a rapid-quench instrument (model QFM-400; Bio-Logic Science Instruments, Claix, France), with reaction times ranging from 10 ms to 6 s.[56,57] For the incorporation of dTTP and dCTP, reactions were performed at 37 °C by mixing 12 μl of a solution containing 100 nM (active sites) of the corresponding RT and 200 nM of the template/primer (31T/21P or 31C/21P, depending on the experiment) in RT buffer [50 mM Tris–HCl (pH 8.0) and 50 mM KCl] with 12 μl of RT buffer containing variable amounts of dNTP in 25 mM $MgCl_2$. Reactions involving AZTTP were conducted under the same conditions with excess concentrations of enzyme (200 nM) over the template/primer duplex (100 nM). These RT and template/primer concentrations were chosen to eliminate the influence of the enzyme turnover rate (k_{ss}), which interferes with the measurement of low incorporation rates. All reactions were stopped with 0.3 M ethylenediaminetetraacetic acid (EDTA) (final concentration).

For 3TCTP, the reaction times were within the range of 10 s–5 min, and the RT was included in the assay at a final concentration of 300 nM. These incubations were carried out manually by mixing 5 μl of RT buffer containing the RT and the template/primer, and 5 μl of the same buffer containing the dNTP and $MgCl_2$. At appropriate times, 10 μl of stop solution [10 mM EDTA in 90% (vol/vol) formamide containing 3 mg/ml xylene cyanol FF and 3 mg/ml bromophenol blue] was added to the reaction. Products were analyzed by sequencing gel electrophoresis [20% (wt/vol) polyacrylamide/8 M urea in Tris–borate–EDTA buffer] and quantified by phosphorimaging with a BAS 1500 scanner (Fuji) using the program Tina, version 2.09 (Raytest Isotopenmessgerate Gmbh, Staubenhardt, Germany). The formation of product [P] over time was fitted with a burst equation:

$$[P] = A[1 - \exp(-k_{obs}t)] + k_{ss}t$$

where A is the amplitude of the burst, k_{obs} is the apparent kinetic constant of the formation of the phosphodiester bond, and k_{ss} is the enzyme turnover rate, which is the kinetic constant of the steady-state linear phase. The dependence of k_{obs} on dNTP concentration is described by the hyperbolic equation:

$$k_{obs} = k_{pol}[\text{dNTP}]/(K_d + [\text{dNTP}])$$

where K_d and k_{pol} are the equilibrium and catalytic rate constants of the dNTP for RT, respectively. K_d and k_{pol} were determined from curve fitting using Sigma Plot.

Steady-state kinetic assays

Nucleotide incorporation reactions were performed by mixing 20 μl of a solution containing 24–80 nM (active sites) of the corresponding RT and 200 nM of the template/primer 31T/21P in RT buffer with 20 μl of RT buffer containing different concentrations of dNTP (in the range of 0.015–500 μM) in the presence of 25 mM $MgCl_2$. After the samples had been incubated at 37 °C for 10, 20, 30, and 40 s, aliquots of 8 μl were removed and added to 8 μl of EDTA-containing stop solution. Products were then resolved on denaturing polyacrylamide–urea gels, and the rate of product formation was determined by phosphorimaging. The rate of product formation was measured for 10–12 different concentrations of AZTTP or dTTP, and the catalytic constants k_{cat} and K_m were determined after fitting the elongation data to the Michaelis–Menten equation.

Foscarnet inhibition was determined after measuring the amount of elongated primer in reactions carried out in RT buffer containing 5 μM dTTP for 0–30 s in the presence of different concentrations of inhibitor (0–5 mM). Incubation times were within the linear range of the corresponding time course. The amount of primer extension products was plotted *versus* the foscarnet concentration, and the data were fitted to a hyperbola to obtain the corresponding IC_{50} value.

Chain terminator excision assays

RT-catalyzed DNA rescue reactions were performed with D38/25PGA or D38G/25PGG DNA duplexes following a described procedure.[15,20] Briefly, the DNA duplex containing the phosphorylated primer (60 nM) and the corresponding RT were preincubated at 37 °C for 10 min in 20 μl of 50 mM Hepes buffer (pH 7.0) containing 15 mM NaCl, 15 mM magnesium acetate, 130 mM potassium acetate, 1 mM dithiothreitol, and 5% (wt/vol) polyethylene glycol 6000. Reactions were initiated by adding 20 μl of preincubation buffer containing 50 μM AZTTP or 200 μM 3TCTP, depending on the assay. After the samples had been incubated at 37 °C for 30 min, the rescue reactions were carried out by adding 40 μl to a mixture of all dNTPs and the corresponding PPi donor in the buffer indicated above. The final concentration of sodium PPi was 20 or 200 μM, depending on the assay, while ATP was supplied at 3.2 mM. Rescue reactions were carried out in the presence of a 100 μM concentration of each dNTP, except for the next complementary dNTP (dATP, under our assay conditions) that was supplied at 1 μM. This lower concentration was necessary to minimize its inhibitory effects on the efficiency of the rescue reactions. Active RT concentrations in these assays were within the range of 20–60 nM. Rescue reactions were incubated for up to 2 h, and aliquots of 4 μl were removed at appropriate times and added to 12 μl of EDTA-containing stop solution. Products were then resolved on denaturing polyacrylamide–urea gels, and primer rescue was quantified by phosphorimaging.

The inhibitory effect of dATP was determined after measuring the amount of rescued primer in reactions carried out for 0–5 min in the presence of different concentrations of dATP. In these experiments, incubation times were within the linear range of the corresponding time course.

Recombinant virus and drug susceptibility tests

These assays were performed as described,[18,58] using viral clones described by Villena *et al.*[38] Briefly, HIV-1 drug susceptibility data were obtained after infecting 35,000 MT-4 cells with one hundred 50% tissue culture infective doses of virus (at a multiplicity of infection of 0.003) by exposing the HIV-1-infected cultures to various concentrations of each drug (fivefold dilutions). After MT-4 cells had been allowed to proliferate for 5 days, the number of viable cells was determined using a tetrazolium-based colorimetric method.

Homology modeling and molecular dynamics simulations

A structural model of mutant Δ69 RT was constructed by standard homology modeling techniques using the SWISS-MODEL server.[59] The coordinates of the wild-type RT in the ternary complex of HIV-1 RT/double-stranded DNA/dTTP (Protein Data Bank file 1RTD)[39] were used as template. The structural quality of the model was checked using WHAT-CHECK routines[60] from the WHAT IF program,[61] and the PROCHECK validation program from the SWISS-MODEL server facilities.[59] In order to optimize geometries and to release local constraints or inappropriate contacts, the modeled structure was energy minimized with the implementation of the GROMOS 43B1 force field in the program DeepView,[62] using 500 steps of steepest-descent minimization, followed by 500 steps of conjugate-gradient minimization.

Molecular dynamics simulations, based on the model, were performed as previously described for the wild-type HIV-1 RT.[40] The system included the DNA polymerase domain (residues 1–389) of the 66-kDa subunit of HIV-1 Δ69 RT, a 15/12-mer DNA/DNA template/primer, and residues 3–82 of the 51-kDa subunit of the RT. Two Mg^{2+} and the incoming dNTP were also included in the system. The total simulation length was around 10 ns, and the analysis of trajectories was performed as described.[40]

Acknowledgements

We thank the Centro de Investigaciones Energéticas, Medioambientales y Tecnológicas (Madrid) for a generous allowance of computer time on their SGI servers. This study was supported by the Fundación para la Investigación y Prevención del SIDA en España (grant 36523/05), the Instituto de Salud Carlos III through the Red Temática de Investigación Cooperativa en SIDA (RD06/0006/0025), and the Spanish Ministry of Education and Science (grant BIO2007-60319). An institutional grant of Fundación Ramón Areces to the Centro de Biología Molecular "Severo Ochoa" is also acknowledged.

References

1. Castro, H. C., Loureiro, N. I. V., Pujol-Luz, M., Souza, A. M. T., Albuquerque, M. G., Santos, D. O. *et al.* (2006). HIV-1 reverse transcriptase: a therapeutical target in the spotlight. *Curr. Med. Chem.* **13**, 313–324.
2. Basavapathruni, A. & Anderson, K. S. (2007). Reverse transcription of the HIV-1 pandemic. *FASEB J.* **21**, 3795–3808.
3. Vivet-Boudou, V., Didierjean, J., Isel, C. & Marquet, R. (2006). Nucleoside and nucleotide inhibitors of HIV-1 replication. *Cell. Mol. Life Sci.* **63**, 163–186.
4. Menéndez-Arias, L. (2008). Mechanisms of resistance to nucleoside analogue inhibitors of HIV-1 reverse transcriptase. *Virus Res.* **134**, 124–146.
5. Sluis-Cremer, N. & Tachedjian, G. (2008). Mechanisms of inhibition of HIV replication by non-nucleoside reverse transcriptase inhibitors. *Virus Res.* **134**, 147–156.
6. Ren, J. & Stammers, D. K. (2008). Structural basis for drug resistance mechanisms for non-nucleoside inhibitors of HIV reverse transcriptase. *Virus Res.* **134**, 157–170.
7. Sarafianos, S. G., Das, K., Clark, A. D., Jr, Ding, J., Boyer, P. L., Hughes, S. H. & Arnold, E. (1999). Lamivudine (3TC) resistance in HIV-1 reverse transcriptase involves steric hindrance with β-branched amino acids. *Proc. Natl Acad. Sci. USA*, **96**, 10027–10032.
8. Deval, J., Selmi, B., Boretto, J., Egloff, M. P., Guerreiro, C., Sarfati, S. & Canard, B. (2002). The molecular mechanism of multidrug resistance by the Q151M human immunodeficiency virus type 1 reverse transcriptase and its suppression using α-boranophosphate nucleotide analogues. *J. Biol. Chem.* **277**, 42097–42104.
9. Deval, J., Alvarez, K., Selmi, B., Bermond, M., Boretto, J., Guerreiro, C. *et al.* (2005). Mechanistic insights into the suppression of drug resistance by human immunodeficiency virus type 1 reverse transcriptase using α-boranophosphate nucleoside analogs. *J. Biol. Chem.* **280**, 3838–3846.
10. Ray, A. S., Basavapathruni, A. & Anderson, K. S. (2002). Mechanistic studies to understand the progressive development of resistance in human immunodeficiency virus type 1 reverse transcriptase to abacavir. *J. Biol. Chem.* **277**, 40479–40490.
11. Arion, D., Kaushik, N., McCormick, S., Borkow, G. & Parniak, M. A. (1998). Phenotypic mechanism of HIV-1 resistance to 3′-azido-3′-deoxythymidine (AZT): increased polymerization processivity and enhanced sensitivity to pyrophosphate of the mutant viral reverse transcriptase. *Biochemistry*, **37**, 15908–15917.
12. Meyer, P. R., Matsuura, S. E., Mian, A. M., So, A. G. & Scott, W. A. (1999). A mechanism of AZT resistance: an increase in nucleotide-dependent primer unblocking by mutant HIV-1 reverse transcriptase. *Mol. Cell*, **4**, 35–43.
13. Meyer, P. R., Matsuura, S. E., Schinazi, R. F., So, A. G. & Scott, W. A. (2000). Differential removal of thymidine nucleotide analogues from blocked DNA chains by human immunodeficiency virus reverse transcriptase in the presence of physiological concentrations of 2′-deoxynucleoside triphosphates. *Antimicrob. Agents Chemother.* **44**, 3465–3472.
14. Boyer, P. L., Sarafianos, S. G., Arnold, E. & Hughes, S. H. (2001). Selective excision of AZTMP by drug-resistant human immunodeficiency virus reverse transcriptase. *J. Virol.* **75**, 4832–4842.
15. Mas, A., Vázquez-Álvarez, B. M., Domingo, E. & Menéndez-Arias, L. (2002). Multidrug-resistant HIV-1 reverse transcriptase: involvement of ribonucleotide-dependent phosphorolysis in cross-resistance to nucleoside analogue inhibitors. *J. Mol. Biol.* **323**, 181–197.
16. Shirasaka, T., Kavlick, M. F., Ueno, T., Gao, W.-Y., Kojima, E., Alcaide, M. L. *et al.* (1995). Emergence of human immunodeficiency virus type 1 variants with resistance to multiple dideoxynucleosides in patients receiving therapy with dideoxynucleosides. *Proc. Natl Acad. Sci. USA*, **92**, 2398–2402.
17. Iversen, A. K. N., Shafer, R. W., Wehrly, K., Winters, M. A., Mullins, J. I., Chesebro, B. & Merigan, T. C. (1996). Multidrug-resistant human immunodeficiency virus type 1 strains resulting from combination antiretroviral therapy. *J. Virol.* **70**, 1086–1090.
18. Mas, A., Parera, M., Briones, C., Soriano, V., Martínez, M. A., Domingo, E. & Menéndez-Arias, L. (2000). Role of a dipeptide insertion between codons 69 and 70 of HIV-1 reverse transcriptase in the mechanism of AZT resistance. *EMBO J.* **19**, 5752–5761.
19. Matamoros, T., Franco, S., Vázquez-Álvarez, B. M., Mas, A., Martínez, M. A. & Menéndez-Arias, L. (2004).

Molecular determinants of multi-nucleoside analogue resistance in HIV-1 reverse transcriptases containing a dipeptide insertion in the fingers subdomain. Effect of mutations D67N and T215Y on removal of thymidine nucleotide analogues from blocked DNA primers. *J. Biol. Chem.* **279**, 24569–24577.
20. Cases-González, C. E., Franco, S., Martínez, M. A. & Menéndez-Arias, L. (2007). Mutational patterns associated with the 69 insertion complex in multi-drug-resistant HIV-1 reverse transcriptase that confer increased excision activity and high-level resistance to zidovudine. *J. Mol. Biol.* **365**, 298–309.
21. Menéndez-Arias, L., Matamoros, T. & Cases-González, C. E. (2006). Insertions and deletions in HIV-1 reverse transcriptase: consequences for drug resistance and viral fitness. *Curr. Pharm. Des.* **12**, 1811–1825.
22. Eggink, D., Huigen, M. C. D. G., Boucher, C. A. B., Götte, M. & Nijhuis, M. (2007). Insertions in the β3–β4 loop of reverse transcriptase of human immunodeficiency virus type 1 and their mechanism of action, influence on drug susceptibility and viral replication capacity. *Antiviral Res.* **75**, 93–103.
23. Winters, M. A., Coolley, K. L., Girard, Y. A., Levee, D. J., Hamdan, H., Shafer, R. W. *et al.* (1998). A 6-basepair insert in the reverse transcriptase gene of human immunodeficiency virus type 1 confers resistance to multiple nucleoside inhibitors. *J. Clin. Invest.* **102**, 1769–1775.
24. Sugiura, W., Matsuda, M., Matsuda, Z., Abumi, H., Okano, A., Oishi, T. *et al.* (1999). Identification of insertion mutations in HIV-1 reverse transcriptase causing multiple drug resistance to nucleoside analogue reverse transcriptase inhibitors. *J. Hum. Virol.* **2**, 146–153.
25. Yahi, N., Tamalet, C., Tourrès, C., Tivoli, N., Ariasi, F., Volot, F. *et al.* (1999). Mutation patterns of the reverse transcriptase and protease genes in human immunodeficiency virus type 1-infected patients undergoing combination therapy: survey of 787 sequences. *J. Clin. Microbiol.* **37**, 4099–4106.
26. Van Vaerenbergh, K., van Laethem, K., Albert, J., Boucher, C. A. B., Clotet, B., Floridia, M. *et al.* (2000). Prevalence and characteristics of multinucleoside-resistant human immunodeficiency virus type 1 among European patients receiving combinations of nucleoside analogues. *Antimicrob. Agents Chemother.* **44**, 2109–2117.
27. Briones, C., Mas, A., Pérez-Olmeda, M., Altisent, C., Domingo, E. & Soriano, V. (2001). Prevalence and genetic heterogeneity of the reverse transcriptase T69S-S-X insertion in pretreated HIV-infected patients. *Intervirology*, **44**, 339–343.
28. Masquelier, B., Race, E., Tamalet, C., Descamps, D., Izopet, J., Buffet-Janvresse, C. *et al.* (2001). Genotypic and phenotypic resistance patterns of human immunodeficiency virus type 1 variants with insertions or deletions in the reverse transcriptase (RT): multicenter study of patients treated with RT inhibitors. *Antimicrob. Agents Chemother.* **45**, 1836–1842.
29. Imamichi, T., Sinha, T., Imamichi, H., Zhang, Y. M., Metcalf, J. A., Falloon, J. & Lane, H. C. (2000). High-level resistance to 3′-azido-3′-deoxythymidine due to a deletion in the reverse transcriptase gene of human immunodeficiency virus type 1. *J. Virol.* **74**, 1023–1028.
30. Ross, L., Johnson, M., Ferris, R. G., Short, S. A., Boone, L. R., Melby, T. E. *et al.* (2000). Deletions in the β3–β4 hairpin loop of HIV-1 reverse transcriptase are observed in HIV-1 isolated from subjects during long-term antiretroviral therapy. *J. Hum. Virol.* **3**, 144–149.
31. Tamalet, C., Yahi, N., Tourrès, C., Colson, P., Quinson, A. M., Poizot-Martin, I. *et al.* (2000). Multidrug resistance genotypes (insertions in the β3–β4 finger subdomain and MDR mutations) of HIV-1 reverse transcriptase from extensively treated patients: incidence and association with other resistance mutations. *Virology*, **270**, 310–316.
32. Imamichi, T., Murphy, M. A., Imamichi, H. & Lane, H. C. (2001). Amino acid deletion at codon 67 and Thr-to-Gly change at codon 69 of human immunodeficiency virus type 1 reverse transcriptase confer novel drug resistance profiles. *J. Virol.* **75**, 3988–3992.
33. Boyer, P. L., Imamichi, T., Sarafianos, S. G., Arnold, E. & Hughes, S. H. (2004). Effects of the Δ67 complex of mutations in human immunodeficiency virus type 1 reverse transcriptase on nucleoside analog excision. *J. Virol.* **78**, 9987–9997.
34. Winters, M. A., Coolley, K. L., Cheng, P., Girard, Y. A., Hamdan, H., Kovari, L. C. & Merigan, T. C. (2000). Genotypic, phenotypic, and modeling studies of a deletion in the β3–β4 region of the human immunodeficiency virus type 1 reverse transcriptase gene that is associated with resistance to nucleoside reverse transcriptase inhibitors. *J. Virol.* **74**, 10707–10713.
35. Suzuki, K., Kaufmann, G. R., Mukaide, M., Cunningham, P., Harris, C., Leas, L. *et al.* (2001). Novel deletion of HIV type 1 reverse transcriptase residue 69 conferring selective high-level resistance to nevirapine. *AIDS Res. Hum. Retroviruses*, **17**, 1293–1296.
36. Winters, M. A. & Merigan, T. C. (2001). Variants other than aspartic acid at codon 69 of the human immunodeficiency virus type 1 reverse transcriptase gene affect susceptibility to nucleoside analogs. *Antimicrob. Agents Chemother.* **45**, 2276–2279.
37. Baxter, J. D., Schapiro, J. M., Boucher, C. A. B., Kohlbrenner, V. M., Hall, D. B., Scherer, J. R. & Mayers, D. L. (2006). Genotypic changes in human immunodeficiency virus type 1 protease associated with reduced susceptibility and virologic response to the protease inhibitor tipranavir. *J. Virol.* **80**, 10794–10801.
38. Villena, C., Prado, J. G., Puertas, M. C., Martínez, M. A., Clotet, B., Ruiz, L. *et al.* (2007). Relative fitness and replication capacity of a multinucleoside analogue-resistant clinical human immunodeficiency virus type 1 isolate with a deletion of codon 69 in the reverse transcriptase coding region. *J. Virol.* **81**, 4713–4721.
39. Huang, H., Chopra, R., Verdine, G. L. & Harrison, S. C. (1998). Structure of a covalently trapped catalytic complex of HIV-1 reverse transcriptase: implications for drug resistance. *Science*, **282**, 1669–1675.
40. Mendieta, J., Cases-González, C. E., Matamoros, T., Ramírez, G. & Menéndez-Arias, L. (2008). A Mg^{2+}-induced conformational switch rendering a competent DNA polymerase catalytic complex. *Proteins*, **71**, 565–574.
41. Olivares, I., Mulky, A., Boross, P. I., Tözsér, J., Kappes, J. C., López-Galíndez, C. & Menéndez-Arias, L. (2007). HIV-1 protease dimer interface mutations that compensate for viral reverse transcriptase instability in infectious virions. *J. Mol. Biol.* **372**, 369–381.
42. Rhee, S. Y., Fessel, W. J., Zolopa, A. R., Hurley, L., Liu, T., Taylor, J. *et al.* (2005). HIV-1 protease and reverse-transcriptase mutations: correlations with antiretroviral therapy in subtype B isolates and implications for drug-resistance surveillance. *J. Infect. Dis.* **192**, 456–465.
43. Weber, J., Chakraborty, B., Weberova, J., Miller, M. D. & Quiñones-Mateu, M. E. (2005). Diminished replicative fitness of primary human immunodeficiency virus

type 1 isolates harboring the K65R mutation. *J. Clin. Microbiol.* **43**, 1395–1400.
44. De Sá Filho, D. J., Sucupira, M. C. A., Caseiro, M. M., Sabino, E. C., Diaz, R. S. & Janini, L. M. (2006). Identification of two HIV type 1 circulating recombinant forms in Brazil. *AIDS Res. Hum. Retroviruses*, **22**, 1–13.
45. Tuske, S., Sarafianos, S. G., Clark, A. D., Jr, Ding, J., Naeger, L. K., White, K. L. *et al.* (2004). Structures of HIV-1 RT–DNA complexes before and after incorporation of the anti-AIDS drug tenofovir. *Nat. Struct. Mol. Biol.* **11**, 469–474.
46. Krebs, R., Immendörfer, U., Thrall, S. H., Wöhrl, B. M. & Goody, R. S. (1997). Single-step kinetics of HIV-1 reverse transcriptase mutants responsible for virus resistance to nucleoside inhibitors zidovudine and 3-TC. *Biochemistry*, **36**, 10292–10300.
47. Feng, J. Y., Shi, J., Schinazi, R. F. & Anderson, K. S. (1999). Mechanistic studies show that (−)-FTP-TP is a better inhibitor of HIV-1 reverse transcriptase than 3TC-TP. *FASEB J.* **13**, 1511–1517.
48. Deval, J., White, K. L., Miller, M. D., Parkin, N. T., Courcambeck, J., Halfon, P. *et al.* (2004). Mechanistic basis for reduced viral and enzymatic fitness of HIV-1 reverse transcriptase containing both K65R and M184V mutations. *J. Biol. Chem.* **279**, 509–516.
49. Isel, C., Ehresmann, C., Walter, P., Ehresmann, B. & Marquet, R. (2001). The emergence of different resistance mechanisms toward nucleoside inhibitors is explained by the properties of the wild type HIV-1 reverse transcriptase. *J. Biol. Chem.* **276**, 48725–48732.
50. Götte, M., Arion, D., Parniak, M. A. & Wainberg, M. A. (2000). The M184V mutation in the reverse transcriptase of human immunodeficiency virus type 1 impairs rescue of chain-terminated DNA synthesis. *J. Virol.* **74**, 3579–3585.
51. Smith, A. J., Meyer, P. R., Asthana, D., Ashman, M. R. & Scott, W. A. (2005). Intracellular substrates for the primer-unblocking reaction by human immunodeficiency virus type 1 reverse transcriptase: detection and quantitation in extracts from quiescent- and activated-lymphocyte subpopulations. *Antimicrob. Agents Chemother.* **49**, 1761–1769.
52. Meyer, P. R., Matsuura, S. E., Zonarich, D., Chopra, R. R., Pendarvis, E., Bazmi, H. Z. *et al.* (2003). Relationship between 3′-azido-3′-deoxythymidine resistance and primer unblocking activity in foscarnet-resistant mutants of human immunodeficiency virus type 1 reverse transcriptase. *J. Virol.* **77**, 6127–6137.
53. Cruchaga, C., Ansó, E., Rouzaut, A. & Martínez-Irujo, J. J. (2006). Selective excision of chain-terminating nucleotides by HIV-1 reverse transcriptase with phosphonoformate as substrate. *J. Biol. Chem.* **281**, 27744–27752.
54. Matamoros, T., Deval, J., Guerreiro, C., Mulard, L., Canard, B. & Menéndez-Arias, L. (2005). Suppression of multidrug-resistant HIV-1 reverse transcriptase primer unblocking activity by α-phosphate-modified thymidine analogues. *J. Mol. Biol.* **349**, 451–463.
55. Boretto, J., Longhi, S., Navarro, J.-M., Selmi, B., Sire, J. & Canard, B. (2001). An integrated system to study multiply substituted human immunodeficiency virus type 1 reverse transcriptase. *Anal. Biochem.* **292**, 139–147.
56. Kati, W. M., Johnson, K. A., Jerva, L. F. & Anderson, K. S. (1992). Mechanism and fidelity of HIV reverse transcriptase. *J. Biol. Chem.* **267**, 25988–25997.
57. Matamoros, T., Kim, B. & Menéndez-Arias, L. (2008). Mechanistic insights into the role of Val75 of HIV-1 reverse transcriptase in misinsertion and mispair extension fidelity of DNA synthesis. *J. Mol. Biol.* **375**, 1234–1248.
58. Kellam, P. & Larder, B. A. (1994). Recombinant virus assay: a rapid, phenotypic assay for assessment of drug susceptibility of human immunodeficiency virus type 1 isolates. *Antimicrob. Agents Chemother.* **38**, 23–30.
59. Arnold, K., Bordoli, L., Kopp, J. & Schwede, T. (2006). The SWISS-MODEL Workspace: a web-based environment for protein structure homology modelling. *Bioinformatics*, **22**, 195–201.
60. Hooft, R. W. W., Vriend, G., Sander, C. & Abola, E. E. (1996). Errors in protein structures. *Nature*, **381**, 272.
61. Vriend, G. (1990). WHAT IF: a molecular modeling and drug design program. *J. Mol. Graphics*, **8**, 52–56.
62. Guex, N. & Peitsch, M. C. (1997). SWISS-MODEL and the Swiss-PdbViewer: an environment for comparative protein modelling. *Electrophoresis*, **18**, 2714–2723.